IMPACT RESPONSE AND PARAMETRIC STUDIES OF REINFORCED CONCRETE CIRCULAR COLUMNS

Thilakarathna H.M.I., School of Urban Development, Queensland University of Technology, Australia
Thambiratnam D.P., School of Urban Development, Queensland University of Technology, Australia
Dhanasekar M., School of Urban Development, Queensland University of Technology, Australia
Perera N.J., Robert Bird Group & School of Urban Development, Queensland University of Technology, Australia

Abstract

This paper presents a detailed description of the influence of critical parameters that govern the vulnerability of columns under lateral impact loads. Numerical simulations are conducted by using the Finite Element program LS-DYNA, incorporating steel reinforcement, material models and strain rate effects. A simplified method based on impact pulse generated from full scale impact tests is used for impact reconstruction and effects of the various pulse loading parameters are investigated under low to medium velocity impacts. A constitutive material model which can simulate failures under tri-axial state of stresses is used for concrete. Confinement effects are also introduced to the numerical simulation and columns of Grade 30 to 50 concrete under pure axial loading are analysed in detail.

This research confirmed that the vulnerability of the axially loaded columns can be mitigated by reducing the slenderness ratio and concrete grade, and by choosing the design option with a minimal amount of longitudinal steel. Additionally, it is evident that approximately a 50% increase in impact capacity can be gained for columns in medium rise buildings by enhancing the confinement effects alone. Results also indicated that the ductility as well as the mode of failure under impact can be changed with the volumetric ratio of lateral steel. Moreover, to increase the impact capacity of the vulnerable columns, a higher confining stress is required. The general provisions of current design codes do not sufficiently cover this aspect and hence this research will provide additional guidelines to overcome the inadequacies of code provisions.

Keywords: Circular columns, Lateral impact, Damage mitigation, Confinement effects

1 Introduction

This research aims to provide a better understanding of the dynamic behaviour of reinforced concrete columns under lateral impact loads. Interest of previous research mainly was on blast response of columns and hence ways to mitigate damage due to impact have been largely unexplored. The few investigations conducted on laterally impacted columns emphasised the strain rate effects and the confinement effects particularly due to mid span impact [1,2]. However, numerical simulation of shear failure conditions of columns under low height impact remains unexplored. In some instances, the methods used for impact reconstruction were either largely simplified or limited to simulate impact between a specific vehicle and a column [3]. The obvious result was the isolated outcomes applicable only for those particular impact events. Consequently structural design of columns remains on oversimplified equivalent static pressure load design methods.

Recent advancement of numerical simulation as well as constitutive material modelling can be implemented successfully to remove these barriers. These advancements allow complex behaviour of

concrete under tri-axial loading conditions to be modelled to a reasonable accuracy not previously possible. The impact reconstruction is conducted using force pulses applied over an equivalent impacted surface at a particular elevation in order to generate universal results which can be applicable to a general vehicle population over the most common modes of collisions. Effort has also been taken to improve the impact capacity of columns through suitable control of design parameters without relying on external energy absorbers or wrapping. Thus the suggestions are merely based on optimum use of the governing parameters. Concrete grades, mode of failures, strain rate effects and confinement effects are particularly examined in the process. Code provisions and the numerical results are also presented for comparison purposes.

2 Brief introduction to the validation of the numerical model

2.1 Material model

LS-DYNA offers an extensive material library suitable for simulating the impact behaviour of concrete [4]. The material model Concrete_Damage_REL3 is used in this investigation to simulate the concrete since the *unconfined compressive strength* and *density of concrete* are the two parameters that are required in the calibration process [5]. However, the default value of the fracture toughness of the concrete is considerably overestimated and hence the parameter b_2 was adjusted using single element analysis until the value agreed with the corresponding value given in the CPF-FIP model code [6].

Even though the mesh dependency of the fracture toughness can be eliminated by adjusting the value of b_2, effect of mesh topology on crack direction still persists in the numerical simulation. The smeared crack approach has been implemented to overcome this problem. The smeared crack model is based on the idea that concrete generates number of micro cracks at the initial stage of loading which form one or more dominant cracks at a later stage. Each individual crack is not numerically resolved and the model captures the deterioration process through a constitutive relation, thus smearing out the cracks over the continuum. Additionally, the unconfined compressive and tensile tests paths are utilised in the model to implement the rate enhancement effects [5]. This method enhances strength equally along any stress path and the different failure stress states will remain unaffected.

2.2 Validation process and outcomes

Results of the Feyarabend [1] column tests were used in the validation process. The tests simulated a laterally impacted rectangular reinforced concrete column. Under the mid span impact, the column reached near failure conditions. Detail descriptions of the development of the numerical model and validation process can be found in Thilakarathna et al. [6].

The results revealed that the observation of EI-Tawil [3] is effective in simplifying the numerical models of impact reconstructions and hence the connected structure can be excluded from the impact simulation. Additionally, perfect bond between concrete and steel can be assumed for these low velocity impact analyses. In particular, axial load must be applied as a ramped up surface pressure over the section. In other words, the stress controlled methods may be more appropriate in impact simulation as the axial load fluctuation can occur under lateral impact.

3 Parametric studies

3.1 Effects of the Impact Pulse Parameters

Impact pulse parameters play a vital role in the generation of a universal method to determine the vulnerability of columns under all modes of collision. Therefore it is intended to investigate the effects of various pulses generated from full scale vehicles to rigid barrier impact in the impact reconstruction process. In the following phase, the peak force is varied until the columns reach near ultimate stage while keeping the duration as constant in order to account for the various masses and velocities.

The triangular pulse shape is best fitted with the force history diagrams generated from the frontal impact conditions [6]. Sine, Haversine [7], and square formats [8] are the other standard formats used widely to represent the frontal vehicle impacts. However, numerical approaches to determine impact pulse parameters are rare in the literature as collision pulse characteristics depend on the mode of impact, collision partner and vehicle specific parameters. In fact, equations derived based on velocity profile, frontal stiffness, amount of deformation, and restitution may not be applicable to a general vehicle population [9]. In the absence of a precise numerical method to quantify the shape of the collision pulse, basic pulse characteristics are determined based on the observation that the product of the mass and velocity of the impacting vehicle is equal to the area under the force history diagram and the average duration of the typical pulses are assumed to be 100ms based on the experimental impact data relevant to the various masses, stiffness and velocities [6].

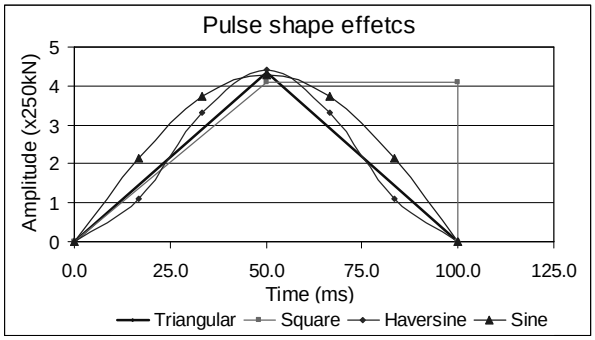

Figure 1: Various iso-damage pulses

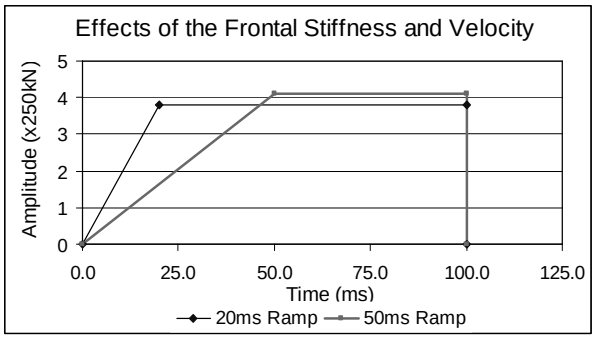

Figure 2: Effects of the strain rate or frontal stiffness

Figure 1 shows the various pulses with different shapes that leads to equivalent damage (Iso-damage) conditions. Triangular and haversine failure amplitudes are almost equal, and the square pulse with equivalent ramp up duration is the one that causes the same damage with minimum peak. Nevertheless, the observed impact behaviour is more sensitive to the peak impact force than the associated impulse similar to quasi-static loading. Apparently, the impact forces belong to the quasi static region. The strain rate sensitivity of the impact can be examined by reducing the slope of the iso-damage function. When the slope of the ramp function is increased the column fails at lower amplitude (see Figure 2) even though triangular force pulses implied the opposite [6]. Consequently, the inertia effects are more predominant than the strain rate effects for rectangular pulses in the quasi-static region. Having provided that the resultant variations are negligible, any of these characteristic curves in vehicle impact generated force history space can be used to define a force-impulse diagram for the impacted columns when the structural damage is controlled by the shear capacity of the section. Additionally, collision severity can be predicted by extrapolating a known collision pulse as the influence of strain rate effect is negligible.

3.2 Impact behaviour of axially loaded column

The impact capacity of typical braced columns of five to twenty storey buildings made of Grade 30 to 50 concrete was investigated using comprehensive numerical simulations. The structural design is based on AS3600 standards [11]. However for comparison purposes axial stresses on the columns are maintained approximately constant for one particular concrete grade rather than axial load on the columns. Two alternative design options with two different steel ratios were examined in the analysis. As far as the area of contact is concerned, EN 1991(2006) suggested that the contact area can be around 0.25m high for car impact [12]. However, there is no guidance on the lateral distribution of the pressure across the section, particularly for circular columns. In this situation experimental results suggest that the effective contact width can be taken as 0.25% of the perimeter if the frictional effects are neglected [6].
Due to the low elevation impact conditions, most of the impacted columns failed in flexural shear failure conditions. Localised stress concentration exceeded the compressive and tensile capacities of the concrete at the contact interface and spall off the concrete cover by reducing the effective area of the column. Under this circumstance, the column fails due to shear initially and flexure subsequently causing collapse. Based on the above observations, it is expected that the parameters that govern flexural shear type failures under quasi-static loading condition can be effectively used to mitigate the damage under impact conditions.

3.3 Effects of the diameter of the column, concrete grade and steel ratio

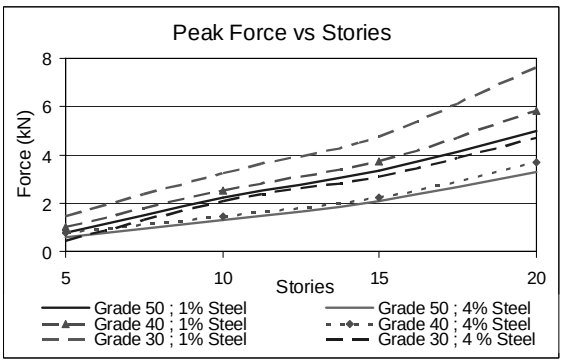

Figure 3: Effects of the diameter of the column

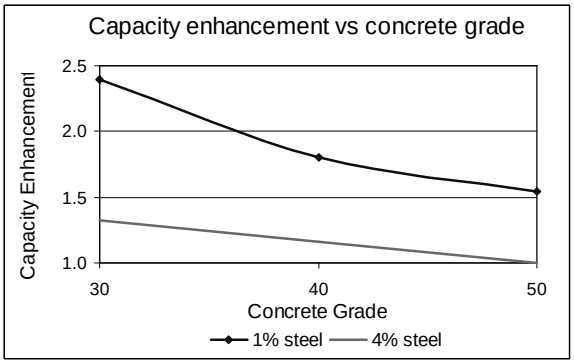

Figure 4: Effects of the concrete grade

Impact capacities of the columns at each storey level and the capacity variation with the grade of concrete are shown in Figure 3 along with the two steel ratios. Concrete grade as well as the steel ratio

has profound effects on the impact capacity of the columns. The equivalent columns made of lower grade concrete improved the impact capacity while columns with a high longitudinal steel ratio decrease the capacity contrary to what would be expected. Comparative average increments of the impact capacities are given in Figure 4 relevant to the Grade 50 concrete column with 4% steel. The diagram clearly exhibits the impact of the steel ratio and the grade of concrete while emphasising the possibility of improving the impact capacity up to 2.4 times by selecting various combinations of concrete grades and longitudinal steel.

4 Finite element analysis of confined circular columns

The simulation was conducted assigning unconfined material characteristics to the cover concrete and enhanced material characteristics to the core concrete to account for the various confinement stresses due to the spiral spacing, diameter of spirals and steel grades. The parametric study is then extended to investigate their individual contribution.

4.1 Stress-strain model for confined concrete

In general, transverse reinforcement confines the compressed concrete and prevents pre-mature buckling of compressed longitudinal bars while acting as shear reinforcement. One of the objectives of this investigation is to quantify the enhancement of the impact capacity due to the transverse reinforcement present in the vulnerable region of the impacted column. The stress-strain model developed by Mander et al. (1988) simulates the confinement effects in this process [13]. It was assumed that the passive lateral confining pressure exerted by the transverse reinforcement leads to a tri-axial state of stress in the core concrete and thus enhances the compressive strength compared to the unconfined concrete. Eventually the equal and opposite forces acting on the lateral reinforcement may rupture the hoops at one stage by bringing the useful ultimate longitudinal compression strain to a residual level (see Figure 5). Longitudinal compression strain of confined concrete within the range of 0.02 to 0.08 should be maintained to satisfy this requirement [14].

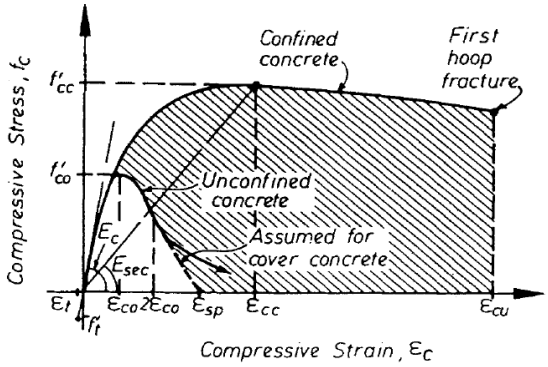

Figure 5: Stress-strain model for confined concrete proposed by Mander at al. (1988)

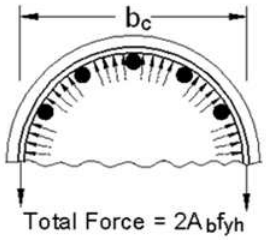

$$f_l = \frac{2A_b f_{yh}}{sb_c}$$

Figure 6: Confining stress provided by the transverse reinforcements [13]

Even though this model was developed under quasi-static loading conditions it allows inclusion of strain rate effects. The lateral confining pressure (f_l) can be found by considering the stability of the half body confined by the transverse hoops as shown in Figure 6. Descriptive details of the stress-strain model can be found in Mander et al. (1988) including the definitions of the relevant notations. In particular, for a section with equal effective lateral confining stress in each direction, the ratio of the compressive strength of the confined concrete f'_{cc} to the comprehensive strength of unconfined concrete f'_{co} is given by,

$$\frac{f'_{cc}}{f'_{co}} = 2.254\sqrt{1+7.94\frac{f'_l}{f'_{co}}} - 2.0\frac{f'_l}{f'_{co}} - 1.254 \qquad \text{Eq : 1}$$

4.2 Applicability of the model under impact conditions

One of the main assumptions of the stress-strain model by Mander at al. (1988) is that the transverse reinforcement reaches its ultimate capacity due the dilation of the concrete core under hydrostatic stress conditions. However, the expansion of the concrete core will not be large under working conditions and hence the tensile capacity of the longitudinal steel will not be fully developed [15]. Nevertheless, concrete can absorb more energy under impact conditions and hence highly localised stresses can be generated in the vicinity of the impact. On the other hand, enhanced tensile strength due to the strain rate reduces the number of cracks while increasing the bond strength between concrete and steel. The improved bond

strength led to stress concentration in the reinforcement [16]. Consequently transverse reinforcement may yield under impact conditions.
Additionally, for stirrup spacing of d/2 the specimens failed in brittle and ductile modes under dynamic and static loading conditions respectively while for stirrup spacing of d/4, the loading rate appeared to have no effect on the failure mode [17]. These are evidence of the confinement effects that can act as a governing factor under the impact conditions. Therefore the above model is valid even under impact conditions.

5 Effects of the confinement

5.1 Behaviour under lateral loads

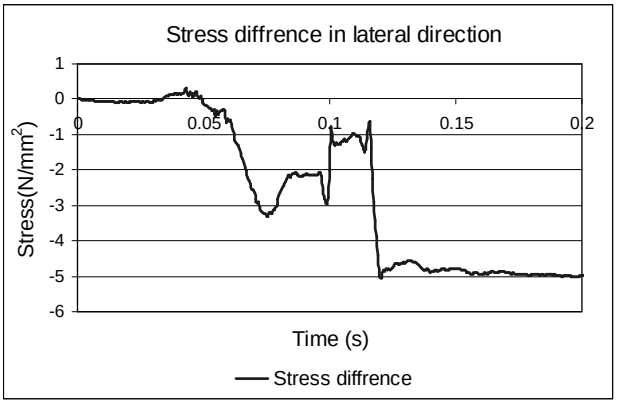

Figure 7: Stress difference at the cover-core interface

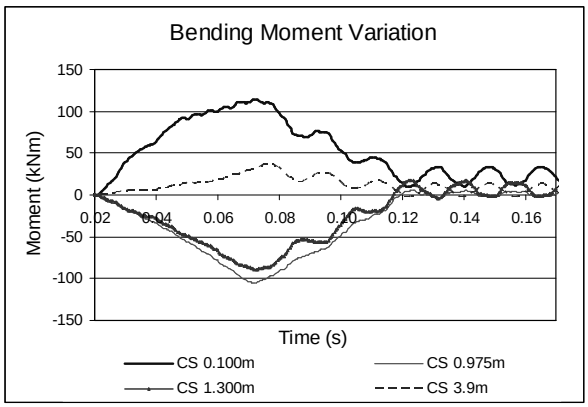

Figure 8: Impact induced bending moments

Figure 7 shows the stress difference generated at the interface of the core and cover concrete at a cracked section close to the bottom support. The 12mm spirals are placed at 100mm spacing in this column (see Figure 9). This arrangement generates higher confinement stresses in the core concrete and hence the resultant stresses in core and cover concrete vary in all directions. The extensive lateral stresses generated at the core-cover interface has exceeded the tensile strength of concrete (See Figure 7). This is one of the reasons why concrete cover fails abruptly during impact. However there is no excessive stress difference under the serviceability conditions which represented by the stresses up to 20ms where the impact begins. The cover concrete in cracked sections did not contribute to the axial capacity of the concrete column at the residual stage. In fact, these sections are the weakest sections which govern the residual capacity of the concrete columns. However the stress difference between cover and core concrete gradually reduced towards the top support as the stress in the vertical direction did not excessively increase in those sections due to impact as shown in Figure 10. This observation also supports the argument that sufficient stress must apply on the core concrete in order to activate the confinement effects.

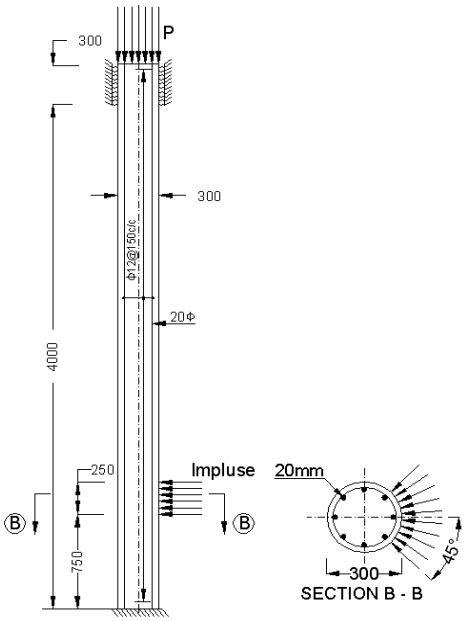

Figure 9: Axial and Lateral load application

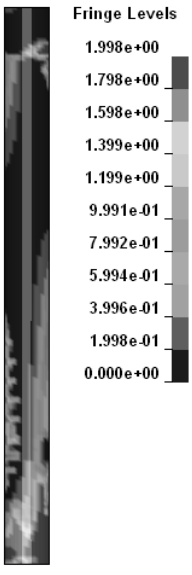

Figure 10: Resultant strain variation in the column

5.2 Bending moment and resultant shear due to impact

Variation of the resultant bending moment due to impact can be measured with 'SECFORC' in LS-DYNA code [4]. The 'SET' option under the 'SECFORC' uses a set of nodes to define a cross section. Forces from the elements belonging to the node set are summed up to form the moment in this method and hence interconnected elements belonging to only one side of the nodes should be defined at one particular section.

The measured moments at each cross section (CS) are given in Figure 8 with the relevant distances measured from the bottom. The highest moments are generated in the vicinity of the impact (0.975m) and close to the support (0.100m), but with opposite signs. The moment is gradually reduced away from the bottom support beyond the point of the impact. However another directional change can be seen close to the top support (3.9m) which signifies the generation of third order vibration mode in the impacted column. Consequently, excessive shear forces are generated at the contraflexure points located close to the supports. This observation may be cited as a potential reason for the failure of the column shown in Figure 11 which indicates typical shear critical situation. It is also important to note that laps forming in this region worsen the consequences. Thus, conventional design and detailing practices, which lead to impact damage, need modification. Laps should be avoided and transverse reinforcement should be provided close to the support where shear strength is vital for survival.

Figure11: Damaged column under vehicle impact

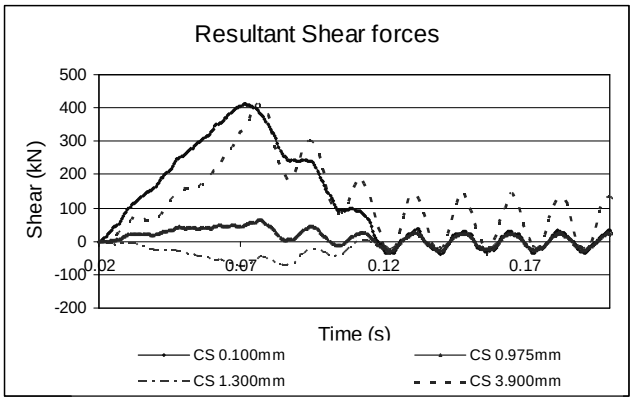

Figure 12: Resultant shear forces

5.3 Effectiveness of confinement under impact loads

Effects of the spiral spacing (s), diameter (d) and yield strength (f_{yh}) are investigated in this section with respect to the inner diameter (d_c) of the columns. 6mm spiral with 350 MPa yield strength at 250mm spacing is used as the datum of the analysis as this arrangement will not be effective in improving the confinement effects. In fact, confinement effects are particularly effective when the spirals are below 100mm spacing. In 350 mm diameter columns, nearly 32% improvement can be achieved by reducing the spiral spacing down to 100mm and it can be further improved up to 44% by reducing the spacing down to 50mm. However this enhancement is limited to 10% for 900 mm diameter columns.

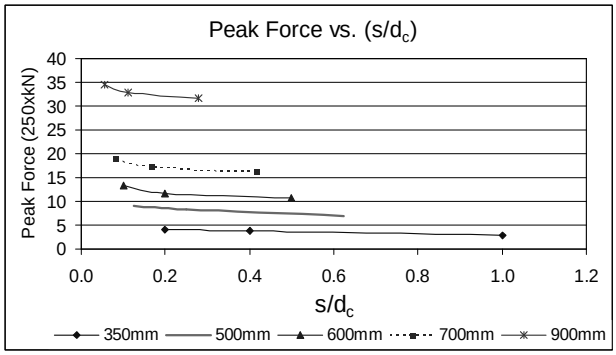

Figure 13: Effectiveness of the confinement for each column

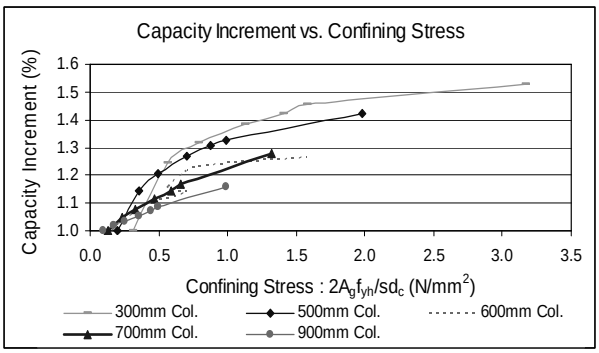

Figure 14: Capacity increment relevant to the confining stress

As far as the effectiveness of the individual parameter is concerned, vulnerability of the column is reduced with the decrease of spiral spacing, increase of the spiral diameter and yield strength. In other words individual or the collective usage of these parameters is possible to enhance the impact capacity of the columns. In particular, provision of spirals with larger diameters is more effective in damage mitigation compared to the reduction of spiral spacing. This observation is effective when the spiral spacing cannot decrease due to practical issues. However the capacity enhancement due to the increment of yield strength of the spirals is negligible. Obviously the highest confinement stress is gained by the small

diameter columns and hence their effectiveness is more pronounced (see Figure 13). Figure 14 describes the inherent relationship between capacity increment and the confining stress, and over 50% increment can be achieved by altering the confinement effect alone as far as the 350 mm diameter columns are concerned. However effectiveness gradually decreased to 12% for 900 mm diameter columns. Consequently, a higher confining stress is required to increase the impact capacity of large diameter columns, than its counter part. Additionally, the effectiveness of the confining stress is further reduced with the increase of the concrete grade and hence the columns made of higher grade concrete need even higher confining stress compared to that of the lower grade concrete. Under these circumstances spiral spacing to be maintained to achieve the required level of confinement under impact loading conditions may be highly under estimated by the general provisions of the codes [11, 18] which are based on maximum diameter of the longitudinal steel.

5.4 Effects on the slenderness ratio

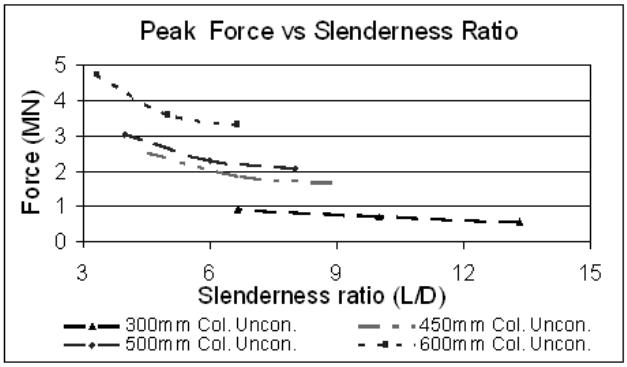

Figure 15: Effect of the slenderness ratio

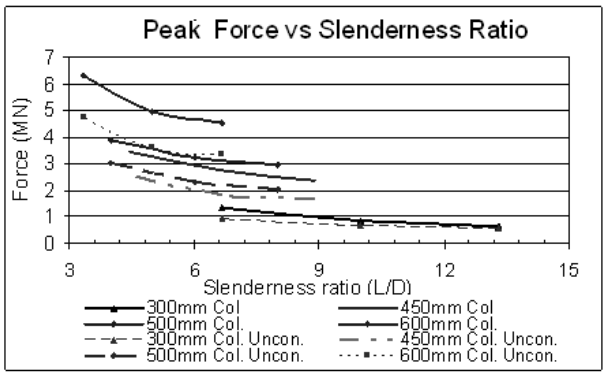

Figure 16: Columns with 12mm links@100mm spacing

Figure 15 shows the impact capacity of the columns with nominal confinement. As the slenderness ratio decreases, the failure plane will change its inclination [6]. Consequently, this change will increase the fracture energy dissipation through the cracked surface while increasing the number of effective spirals in preventing crack propagation. Hence, the investigation continued to examine the impact behaviour of columns under closer spiral spacing.

Capacity enhancement due to the confinement effect is shown in Figure 16 along with the capacities of the columns with nominal confinement. The enhancement is more predominant in larger diameter columns and the average increment of 38% is observed except for 300mm column which shows a lesser increment of about 8 to 20% depending on the effective height. Therefore, the confinement effects may not provide substantial extra capacity particularly to the 300mm diameter short columns. On the other hand 450mm and 500mm diameter columns changed the mode of failure from flexural-shear to flexure even for low slenderness ratios by enhancing the capacity due to the confinement. However, failure mode of 600mm column remains unchanged and hence 500mm is the limiting diameter which changes the response due to the confinement effects.

6 Conclusions

This paper examined the impacte response and capacity enhancement of impacted RC columns by optimum usage of critical parameters inculding the pulse characteristics, concrete grade, steel ratio, slenderness ratio and confinement effects. The main conclusions are summarised below:

1. The default value of the fracture toughness has to be corrected to eliminate the effects of mesh dependency of the finite element model. The stress controlled method is more effective in impact simulation as the axial load can fluctuate under lateral impact.
2. If the duration and the peak force remain identical, the effects of the shape of the pulses are insignificant. Stiffness of the vehicle also has a negligible effect if the pulse characteristics belonging to the vehicle impact generated force history space.
3. Inertia effects are more predominant than the strain rate effects for the square pulses and visa versa is true for triangular pulses even though the comparative advantages are insignificant. Additionally, collision severity can be predicted by extrapolating a known collision pulse as strain rate effect is negligible.
4. Concrete grade as well as the steel ratio has a profound effect on impact capacity of columns. Various combinations of concrete grades and steel ratios will allow impact capacity to be enhanced to 240% if the grade 50 column with 4% steel is considered as the default.

5. Concrete can absorb more energy under impact and dilate core concrete. Tensile strength enhancement under impact will increase the bond strength between steel and concrete. These factors will yield the transverse reinforcements under impact conditions and hence application of the stress-strain model proposed by Mander at al. (1988) in the impact simulation can be justified.
6. Spalling of the cover concrete under impact can be explained using the stress variation in the core-cover interface resulting from the confinement effects. This phenomenon became more obvious in the places where axial stresses increase due to the impact.
7. Resulting bending moment revealed the generation of third mode of vibration in the impacted column and generation of maximum shear forces at contra flexure points close to the supports. Consequently, the impacted column may tend to fail close to the supports under shear critical conditions. Thus, laps should be avoided close to the supports and maximum transverse reinforcement should be provided in the vulnerable regions to avoid shear failures.
8. Confinement effects are particularly effective when the spiral spacing is closer than 100mm. The capacity enhancement could be increased up to 50% and 12% for 350mm and 900mm column respectively by enhancing the confinement effects alone. It is recommended to increase the diameter of the spirals rather than the yield strength when restrictions are applied on minimum allowable spacing of the transverse reinforcement due to practical issues.
9. The provision of lateral reinforcement in structural columns based on maximum diameter of the longitudinal steel is not appropriate for the lateral steel requirement under the impact conditions.
10. Confinement effects may also enhance the impact capacity of column with different slenderness ratios. The enhancements of the capacity in large diameter columns are more predominant as the number of effective spiral increase as the inclination of the failure plain increase with the confinement effects. However, 300mm column shows lesser enhancement due to its lack of sensitivity to the confinement effects in the considered slenderness range.

7 References

[1] Louw, M.J., G. Maritz, and M.J. Loedolff, The Behaviour of RC Columns under Impact Loading, The Civil Engineer in South Africa, 1992: p. 371-378.

[2] Loedolff, M.J., The behaviour of reinforced concrete cantilever columns under lateral impact loads, PhD Thesis, University of Stellenbosch, Sep.1989.

[3] El Tawil, S., E. Severino, and P. Fonseca, *Vehicle Collision with Bridge Piers.* Journal of Bridge Engineering, 2005. 10(3): p. 345-353.

[4] Hallquist, J.O., *LS-DYNA 3D: Theoretical manual, Livermore.* Livermore Software Technological Corporation, 2006.

[5] Malvar, L.J., et al., *A plasticity concrete material model for DYNA3D*, International Journal of Impact Engineering, 1997. 19(9-10): p. 847-873.

[6] Thilakarathna, H.M.I., et al., *Vulnerability of Axially Loaded Columns Subjected to Transverse Impact Loads*, The second infrastructure theme postgraduate conference, 2009. 1(2): p. 22-35

[7] Breed, D.S., V. Castelli, and W.T. Sanders, A New Automobile Crash Sensor Tester. SAE Technical Paper 910655, 1991. Society of automotive engineers, Warrendale, PA.

[8] Varat, M.S. and S.E. Husher, *Crash Pulse Modeling for Vehicle Safety Research*, 18th ESV Paper, Paper 501, USA, 2000.

[9] Brach, R.M., *Mechanical Impact Dynamics*. 1991, New York: John Wiley and Sons Inc.

[10] http://www-nrd.nhtsa.dot.gov/database/nrd-11/veh_db.html

[11] *AS 3600, Concrete structures*, 2004: p. 185.

[12] *EN 1991-1-7:2006, Eurocode 1 - Actions on structures - Part 1-7*: General Actions & Accidental actions. Irish standards, 2006.

[13] Mander, J.B., M.J.N. Priestley, and R. Park, *Theoretical stress-strain model for confined concrete.* Journal of Structural Engineering, ASCE, 1988. 114(8).

[14] Watson, S., F.A. Zahn, and R. Park, *Confining Reinforcement for Concrete Columns.* Journal of Structural Engineering, 1994. 120(6): p. 1798-1824.

[15] Johnny, H.C.M., *Inelastic design of reinforced concrete beams and limited ductile high-strength concrete columns*, PhD Thesis, 2003, University of Hong Kong, Peoples Republic of China.

[16] Memari, A.M., et al., Ductility evaluation for typical existing R /C bridge columns in the eastern USA. Engineering Structures, 2005. 27(2): p. 203-212.

[17] Chung, L. and S.P. Shah, *Effects of loading rate on anchorage bond and beam-column joint.* Structural Journal, 1989. 96(2): p. 132-142.

[18] BS 8110, Part 1: structural use of concrete. British Standards Institution, 1985. London. p. 118.